

BARIUM STRONTIUM TITANATE/EPOXY RESIN NANOCOMPOSITES AS COMPACT ENERGY STORAGE & HARVESTING DEVICES-CONDUCTIVITY ANALYSIS

G. C. Manika*, G. C. Psarras

Smart Materials & Nanodielectrics Laboratory,
Department of Materials Science, University of Patras, 26504, Patras, Greece
(*manikage@upatras.gr)

ABSTRACT

Nanodielectric materials with barium strontium titanate embedded within an epoxy resin matrix were prepared varying the filler content. Broadband dielectric spectroscopy was employed for determining the dielectric response of the specimens. Three relaxation processes appear in all nanocomposites systems: (i) glass to rubber transition (α -mode), (ii) re-arrangement of the polar side groups (β -mode) and (iii) interfacial polarization between systems' constituents. The stored and harvested energies were examined under DC conditions in a voltage range of 10-240V. The coefficient of energy efficiency (n_{eff}) was determined for all filler contents having as parameters the temperature and the applied DC voltage. n_{eff} follows an exponential decay upon temperature for all examined specimens. The highest n_{eff} appears for the 1phr BST at 50V taking the value of 65.9% at 30°C. Finally, the performed conductivity analysis indicates that the conduction process is thermally activated. Both AC and DC conductivity follows an exponential decay upon temperature, indicating the dielectric state of the samples.

1. INTRODUCTION

One of the main problems of the modern society is the energy crisis and related environmental problems, which are mainly derived from the increased energy consumption demands. The exhaustion of fossil fuels in combination with their devastating environmental consequences leads to the need for their immediate replacement. The current energy system is the dominant contributor to the climate change, representing around 60% of total greenhouse gas emissions. Current patterns of energy production and consumption are unsustainable and threaten the environment on both local and global scales. Emissions from the combustion of fossil fuels are the major factors of climate change, and to urban air pollution and acidification of land and water. Renewable energy sources (RES), such as solar, wind and thermal energy can be deal with the modern energy challenges replacing the fossil fuels energy resources with cleaner and renewable ones. Notably, from the 24.5GW of the new capacity built across EU in 2016, the 86% was wind, solar, biomass and water. In addition, another important factor is the improvement of the energy efficiency in current energy systems. The main problem is that most of the produced energy is lost in terms of heat, mainly in electric power generation and transmission, thus it will be crucial to enhance the energy efficiency of the modern energy systems [1-4].

Energy storage refers to the capture of energy generated at one time and consumed later, and energy harvesting is related to self-powered devices that require no external power for operation and thus no replaceable power supplies is needed. So, the introduction of a novel material device which will be able to act as energy storage and harvesting system will be a key objective in meeting the energy challenges of the modern society. Energy materials have received a lot of attention lately due to their potential applicability in a vast number of electronic devices. Multifunctional polymer nanocomposites could be used as structural energy devices, where the matrix and the filler work synergistically for an improved behaviour. Specifically, nanodielectric composites exhibits high energy density which is mainly attributed to the usage of the high dielectric constant filler and high break down strength of the polymer. Ceramic fillers exhibit high values of dielectric permittivity and low breakdown strength, on the other hand, polymers have high dielectric breakdown strength

along with high energy density. Consequently, the combination of both materials results in a composite system with enhanced dielectric properties. The introduction of a system with high dielectric constant and dielectric strength and at the same time without major dielectric loss constitutes a difficult but important task [1, 5-6].

In this work, an insulating epoxy resin was selected as the polymer matrix due to its ease in processing, thermomechanical stability and its relative low cost. Furthermore, ceramic nanoparticles such as the wide band gap BaTiO₃ and SrTiO₃ are considered very promising fillers being able to improve the dielectric properties and the functionality of the system, due to their high permittivity values, and temperature dependent polarization. In addition, the extended interface area and interfacial volume between the polymer matrix and the nanoparticles play a major role in the system's performance. The present study focusses on the determination of the coefficient of energy efficiency of barium strontium titanate /epoxy resin nanocomposite system via the stored and harvested energy, having as parameters the applied DC field, the filler loading and temperature. Finally, conductivity analysis was performed in both AC and DC conditions.

2. EXPERIMENTAL

2.1 Materials and nanocomposite fabrication

The specimens were manufactured by employing commercially available materials. For the preparation of the polymer matrix a low viscosity epoxy resin ER (bishenol-A) with trade mark Epoxol 2004A and cycloaliphatic amine as curing agent with trade name (Epoxol 2004B) were used, which were both provided by Neotex S.A. Athens, Greece. Barium strontium titanate nanoparticles (BaTiO₃/SrTiO₃) BST were purchased by Sigma Aldrich, having a mean particle diameter less than 100nm. The followed procedure includes mixing the resin with the curing agent in a 2:1 (w/w) ratio. As the polymer matrix (ER and hardener) is in liquid state, the ceramic filler was added to produce the nanocomposite specimens. Stirring at a slow rate under ultrasonication was performed in order to avoid the formation of clusters. The homogenized mixtures were poured to moulds and the curing process took place at ambient conditions for a week, followed by post-curing at 100°C for 4h. The content of BST specimens was in parts per hundred resin (phr) per weight and the manufactured samples were: 0, 1, 3, 7, 10, 12 and 15phr.

2.2 Electric measurements

The dielectric characterization was conducted by broadband dielectric spectroscopy (BDS) in the frequency range from 0.1Hz to 10MHz using an Alpha-N- Frequency Response Analyzer supplied by Novocontrol Technologies. The applied V_{rms} was constant at 1V, while the temperature was controlled by Novotherm system (Novocontrol Technologies) with $\pm 0.1^\circ\text{C}$ accuracy. A two-terminal dielectric cell BDS 1200 was used, supplied by Novocontrol. Specimens were placed between the metal electrodes, and isothermal frequency scans were conducted for each examined specimen, from ambient to 160°C with a temperature step of 5°C. Data acquisition was performed automatically in real time via windeta software. All AC measurements were conducted according to the ASTM D150 specifications.

DC measurements were performed via a High-Resistance Meter, DC (Agilent 4339B). Experimental set up includes an automatic measurement process with a test sequence allowing the control and measure the charging and discharging sequence. Data acquisition was fully automated and conducted, in real time via LabView. The applied voltages to all samples were: 10, 50, 100, 150, 200 and 240V. The applied temperatures were: 30, 60, 80, 100 and 120°C. Specimens were put between two electrodes in a parallel plate capacitor configuration. The charging time was 60s for all samples and applied voltages. Prior of every charging-discharging experimental run, was ensured that no stored charges exist in the samples by a discharging and short-circuit procedure. Measurement of the resistance in all samples were conducted at 50, 100 and 200V. For the determination of the DC electrical conductivity the resistance of the samples was measured at 30s time instant. All DC

measurements were performed according to the ASTM D257 specifications.

3. RESULTS AND DISCUSSION

3.1 Dielectric response

Three dimensional dielectric spectra of the real part of dielectric permittivity, loss tangent and AC electrical conductivity as a function of temperature and frequency, for the 12phr BST nanocomposite are presented in Figure 1a, 1b and 1c respectively.

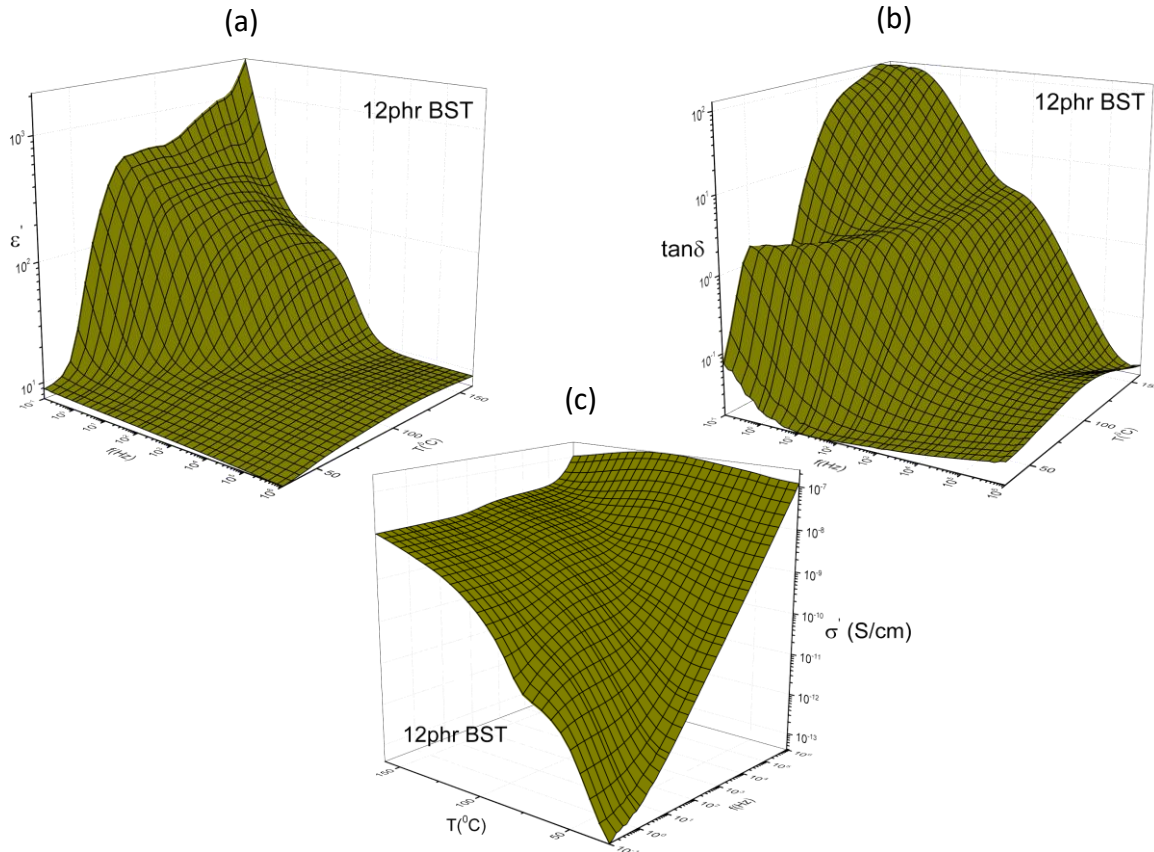


Figure 1. Dielectric spectra of the 12phr BST nanocomposite as a function of temperature and frequency for the: (a) real part of dielectric permittivity, (b) loss tangent and (c) AC conductivity.

Permittivity (ϵ') values increase as the frequency of the applied field diminishes, since dipoles attain sufficient time to orient themselves in the direction of the field. While frequency increases the dipoles fail to follow the rapid alternation of the field, leading to low polarization level and permittivity values. Temperature facilitates the polarization process due to the thermal agitation of the dipoles and ϵ' acquires high values in the low frequency and high temperature range. Three relaxations processes are evident in the permittivity spectra (Figure 1a). These relaxation processes are more apparent in the loss tangent spectra (Figure 1b). Three distinct processes can be observed by the formation of loss peaks. The slower process is recorded in the low frequency and high temperature region, is characterized by longer relaxation time, and dielectric losses acquire the highest recorded values. This process is attributed to Interfacial Polarization (IP), also known as Maxwell-Wanger-Sillars (MWS) effect and is related to the accumulation of unbounded charges at the interfaces of the composite, where they form large dipoles. In the intermediate zone, another relaxation process is present (α -relaxation), which is related to the glass to rubber transition of the amorphous polymer matrix. During α -relaxation the amorphous matrix transforms from the state of stiff and rigid polymer to the state of soft and elastomeric performance. The third relaxation process, evident at low temperature and high frequency range is characterized by the shorter relaxation time and is attributed to the re-arrangement of polar side groups of the main polymer chain and is called β -relaxation process. Finally, 3D dielectric spectra of σ_{AC} (Figure 1c) follows “The universality law”:

$$\sigma_{AC}(\omega) = \sigma_{DC} + A(\omega)^s \quad (1)$$

where σ_{DC} is the $\omega \rightarrow 0$ limiting value of $\sigma_{AC}(\omega)$ and A, s are the parameters depending on the temperature and filler content. According to this law at constant temperature $\sigma_{AC}(\omega)$ acquires the constant σ_{DC} value at low frequencies, while at high frequencies σ_{AC} reveals an exponential dependence on frequency [6-8]. Both α -relaxation and β -relaxations are evident in Figure 1c.

Comparative spectra of the real part of dielectric permittivity (ε') as a function of frequency for all specimens at 30°C are shown in Figure 2.

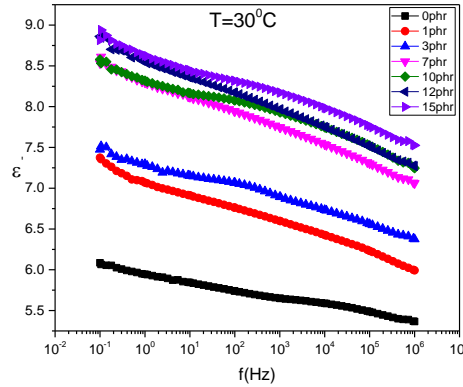


Figure 2. Real part of dielectric permittivity as a function of frequency for all studied BST specimens at 30°C. Figure 2 indicates that ε' values increase with filler content in the whole frequency range, since BST nanoparticles exhibit higher ε' values than epoxy resin. The increase is more noticeable at low frequencies and it is also apparent that the specimen with the highest filler content demonstrates the optimum performance.

3.2 Energy storage and harvesting/Coefficient of energy efficiency

The storing and harvesting procedures were performed by measuring the storing the charging/discharging currents at various voltage levels and at different temperatures. The stored energy is a function of capacitance, which is determined by the geometry of the capacitor and the permittivity of the dielectric material. It is evident through Equation (2) that the only material property which affects capacitance is dielectric permittivity. The external field which is exerted in the dielectric material, leads to the polarization, therefore, the stored energy is calculated via Equation (3).

$$C = \varepsilon \cdot \varepsilon_0 \cdot \frac{A}{d} \quad (2)$$

$$E = \int_0^Q V dq = \frac{1}{2} \cdot \frac{Q^2}{C} \quad (3)$$

where E is the capacitor's energy, Q is the accumulated charge, C the capacitance, ε the dielectric permittivity, A the area of the capacitor's plate, d the distance of the capacitor's parallel plates and ε_0 the dielectric constant of free space. In a nanodielectric system, nanoinclusions operate as a dispersive network of nanocapacitors, being able to store and harvest energy, defining a novel compact material nanodevice. The stored and harvested energies were calculated by integrating the $I = f(t)$ curves, Equation (4), in every case the capacitance of specimen is determined by dielectric measurements at the lowest applied frequency [9-10].

$$E = \frac{1}{2} \cdot \frac{[\int I(t)dt]^2}{C} \quad (4)$$

Figures 3a and 3b present the stored and harvested energies of the 12phr BST nanocomposite at 30°C and 80°C respectively. The systems reinforced by nano BST particles impart to the material enhanced dielectric properties resulting in higher energy efficiency. The elevation of temperature decreases the energy efficiency of the system. The coefficient of energy efficiency (n_{eff}) is defined as the ratio of the discharged upon charged energy, having as parameters the voltage level, the temperature and the time. Both stored and harvested energies were calculated at the same time instant ($t=10s$).

$$n_{eff} = \frac{E_{discharge}}{E_{charge}} \quad (5)$$

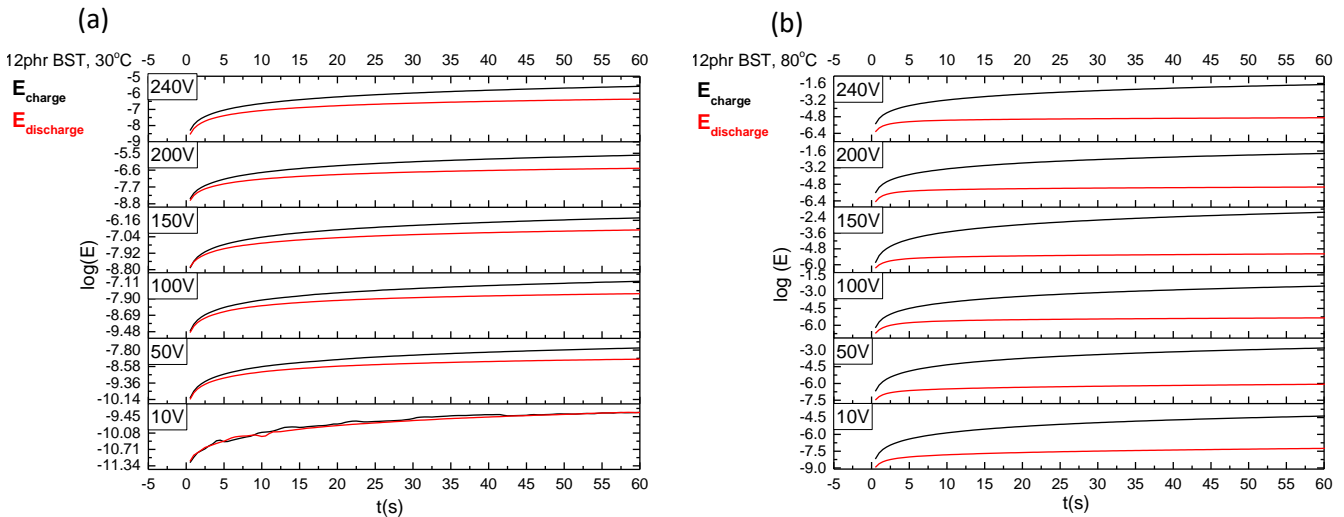


Figure 3. E_{charge} and $E_{discharge}$ as a function of time in all applied DC voltage level for the 12phr BST specimen at (a) 30°C and (b) 80°C.

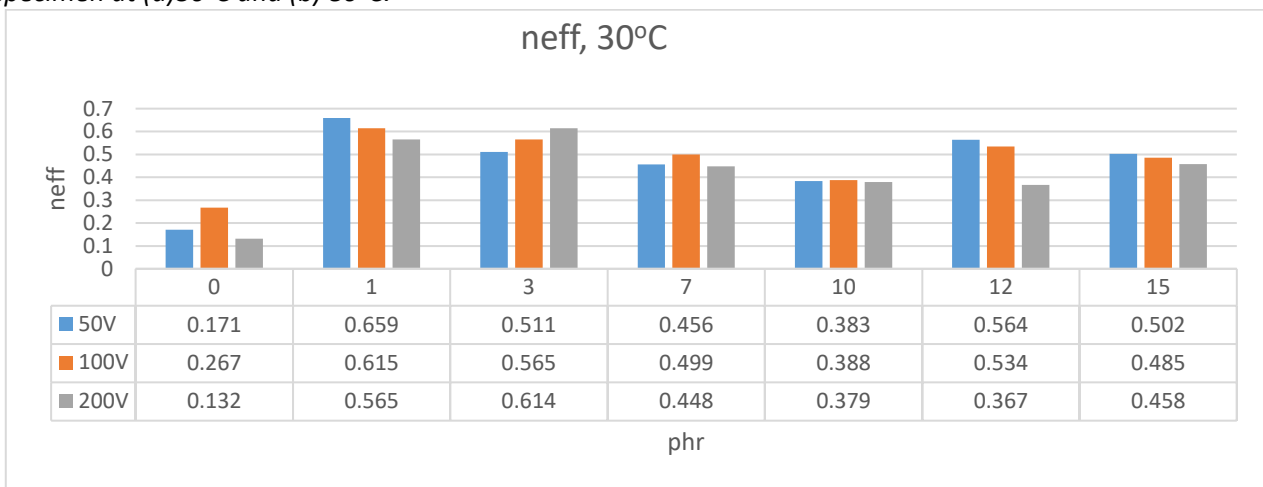


Figure 4. Coefficient of energy efficiency (n_{eff}) at 50, 100 and 200V at 30°C for all BST specimens.

n_{eff} is affected by several factors in a different way, and for this reason it does not follow a systematic pattern. The optimum energy performance at 30°C is displayed by the 1phr BST nanocomposite with $n_{eff}=65.9\%$ at 50V, which basically implies that the amount of the added nanofiller contributes to the heterogeneity of the system and the formation of the extended interface, resulting in lowering the number of space charges which participate in the conduction process. In addition, the effect of the applied voltage is also noticeable. The increase of the applied field influences both the number of injected carriers and the decrease of the potential barriers within the nanocomposites, resulting in easier transportation of charges within the material. The dramatic decrease of n_{eff} upon temperature is attributed to the augment of leakage currents, diminishing thus the stored energy. $n_{eff}(T)$ follows an exponential decay with the form: $n_{eff} = B + Aexp(-KT)$, where B, A and K are material's parameters.

3.3 Conductivity analysis

As conductivity is one of the major electrical properties it was significant to perform conductivity analysis in all BST specimens. Nanocomposites have been manufactured by combing a semiconductive reinforcing phase with a polymer matrix. The calculation of DC conductivity was determined by Equation (6).

$$\sigma_{DC} = \frac{l}{A \cdot R(T)} \tag{6}$$

where l is the average sample thickness, A is the electrode surface (176.625mm^2) and R is the volume resistance of the sample. BST nanoparticles exhibit higher conductivity values in comparison with epoxy resin, resulting in the formation of a network through the polymer matrix leading to

relatively higher conductivity values. A preliminary conductivity study has indicated that σ_{DC} does not follow a systematic pattern as the amount of the reinforcing phase increases. Although σ_{DC} increases dramatically upon temperature, indicating that the conduction process is a thermally activated mechanism. Figure 5a and 5b present the variation of both σ_{DC} and σ_{AC} as function of temperature. There is an exponential dependence in all specimens with a positive temperature coefficient ($\frac{d\sigma}{dT} > 0$). The positive sign of thermal coefficient of conductivity is in accordance with the semiconductive nature of the examined materials and reflects the thermally stimulated random space charge migration within the material. In order the charges to overcome the potential barriers in the polymer matrix composites, they need to acquire sufficient energy which is mainly exerted by temperature [11-12].

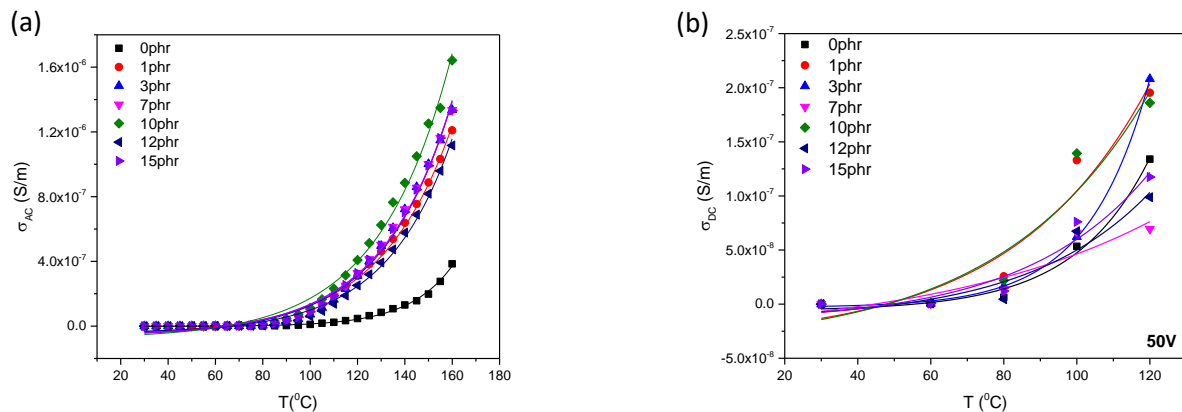


Figure 5. (a) DC conductivity as a function of temperature for all BST specimens at 50v and (b) AC conductivity as a function of temperature at 0.1Hz for all BST specimens.

4. CONCLUSIONS

Nanocomposites consisting of an epoxy resin and barium strontium titanate nanoparticles were fabricated and studied varying the filler content. Electric characterization was conducted via broadband dielectric spectroscopy, revealing three relaxations processes in all dielectric spectra. With descending relaxation time, they are attributed to interfacial polarization, glass to rubber transition (α -relaxation) and re-arrangement of the polar side groups of the polymer matrix (β -relaxation). The ability to store and harvest energy was also investigated under DC conditions. Stored and harvested energies were determined at various temperatures. Coefficient of energy efficiency (n_{eff}) increases with the intergration of the semiconductive filler reaching the highest value of 65.9% for the 1phr BST nanocomposite at 50V. Finally, conductivity study was also performed, both AC and DC conductivity found to increase upon temperature in an exponential way, being in accordance with the dielectric nature of the fabricated systems.

5. REFERENCES

- [1] C. Liu, F. Li, L-P. Ma, H-M. Cheng, *Adv. Energy Mater.* 22 (2010) E28-E62.
- [2] M. Martin-Gonzalez, O. Cabellero-Calero, P. Diaz-Chao, *Renew. Sust. Energ. Rev.*, 24 (2013) 288-305.
- [3] Z.-M. Dang, J.-K. Yuan, S.-H. Yao, R.-J. Liao, *Adv. Mater.*, 25 (2013) 6334-6365.
- [4] AGECC, Report and Recommendations on Energy for Sustainable Future, 28 April 2010, New York.
- [5] G.C. Psarras, *Express Polym. Lett.*, 2(2008) 460.
- [6] G.C. Psarras in *Polymer nanocomposites: Physical properties and applications*, Woodhead Publishing Limited (2010) 31-69.
- [7] O. Vryonis, D.L. Anastasopoulos, A.A. Vradis, G.C. Psarras, *Polymer*. 95 (2016) 82-90.
- [8] A.C. Patsidis, G. C. Psarras, *Smart Mater. Struct.*, 22(2013)115006.
- [9] G.C. Manika, G.C. Psarras, *High Volt.*, 1 (2016) 151-157.
- [10] G. C. Manika, G. C. Psarras, 18th European Conference on Composite Materials, 24-28th June 2018, Athens, Greece.
- [11] G.M. Tsangaris, G.C. Psarras, E. Manolakaki, *Adv. Compos. Lett.*, 8 (1999) 25-29.
- [12] G.C. Psarras, *Sci. Adv. Mater.*, 1 (2009) 101-106.